JOURNAL OF Applied Polymer SCIENCE

# Characterization of multiwalled carbon nanotube filled, palm-oil-based polyalkyds: Effects of loading and *in situ* reaction

**Muhammad Remanul Islam, Mohammad Dalour Hossen Beg, Saidatul Shima Jamari**
Faculty of Chemical and Natural Resources Engineering, Universiti Malaysia Pahang, Lebuhraya Tun Razak, Gambang 26300, Kuantan, Pahang, Malaysia
Correspondence to: M. R. Islam (E-mail: remanraju@yahoo.com) and M. D. H. Beg (E-mail: dhbeg@yahoo.com)

**ABSTRACT:** In this study, the contribution of multiwalled carbon nanotubes (MWCNTs) was studied for the evaluation of the performances of polyalkyd-based films produced from dehydrated palm oil. Initially, different percentages of MWCNTs, including 0.5, 1.0, and 1.5 wt %, were considered for loading into the resin with the help of sonication. Additionally, a 1.0 wt % loading was considered for *in situ* conditions during the esterification process to achieve better dispersion and obtain improved properties of the film. The loading was evaluated by different performance tests, such as those of tensile, elongation, pencil hardness, swelling ratio, gel content, wettability, chemical resistivity, adhesion, and surface morphology. The results of mechanical testing showed that the addition of 1.0 wt % MWCNTs enhanced the tensile strength by 50%, whereas *in situ* conditions were found to be favorable for significantly improving the tensile strength by 75%. Moreover, the wettability, surface morphology, and thermal properties were also found to be in favor of *in situ* conditions for the dispersion of the MWCNTs. © 2015 Wiley Periodicals, Inc. J. Appl. Polym. Sci. **2016**, *133*, 42934.

**KEYWORDS:** biomaterials; biopolymers and renewable polymers; coatings; crosslinking; films

Received 23 May 2015; accepted 14 September 2015
**DOI: 10.1002/app.42934**

## INTRODUCTION

The development of new materials from biobased resources is increasing day by day because of recent concerns for environmental issues and the scarcity of traditional reserved raw materials. A huge mass of biomaterials is available in the surrounding world for exploring value-added products with cost-effective and prominent properties. Among the diverse categories of biomaterials, vegetable oils are promising precursors for different kinds of polymer production.[1] It is noteworthy that the successful utilization of this material for polymer production may reduce the high demand for petroleum, which may be depleted in the near future.[2] Different kinds of plant oils, such as castor, safflower, linseed, mahua, coconut, sunflower, soybean, tung, nahar, and jatropha oils, have been used for the production of various numbers of polymers, such as polyurethane, polyester, poly(ester amide), and epoxy.[1,3,4] Among these polymers, polyesters are being used for surface coatings, paints, adhesives, and composite formulation. Earlier nahar seed, jatropha, and rapeseed oil have been used for alkyd synthesis for different purposes.[5–7] Polyalkyds can be prepared by the reaction of triglycerides, polyols, and acid anhydrides through a two-step process that includes alcoholysis and esterification.[1]

Malaysia produces a huge quantity of palm oil that is basically nondrying in nature and available at low cost. After it is used in food sectors and olechemical industries, the remaining oil can be used for polymer synthesis. Earlier, palm oil was used for the preparation of polyester acrylate resin for wood-coating applications.[8] It was reported as promising candidate for resin preparation for wood-coating applications. In another study that used palm oil for water-reducible acrylic–alkyd resin preparation, it was reported that the product of its modification through an interesterification process with tung oil was suitable for film preparation.[9] The produced films showed excellent water and acid resistivity. Polyalkyds were also prepared from jatropha and rapeseed oil individually for electrical insulation purposes. A comparison was drawn between the properties of the varnishes produced from them, and the rapeseed-oil-based one was found to be superior compared to the other. However, palm-oil-based polyalkyds were prepared, and because of their saturated nature, the drying properties were found to be poor and needed to be improved.[10] Additionally, the mechanical properties of the resins were not up to the level of standard; they were improved in this study. Thus, the aim of our research was to improve the unsaturation of palm oil through a dehydration process. Moreover, to improve the mechanical properties, multiwalled carbon

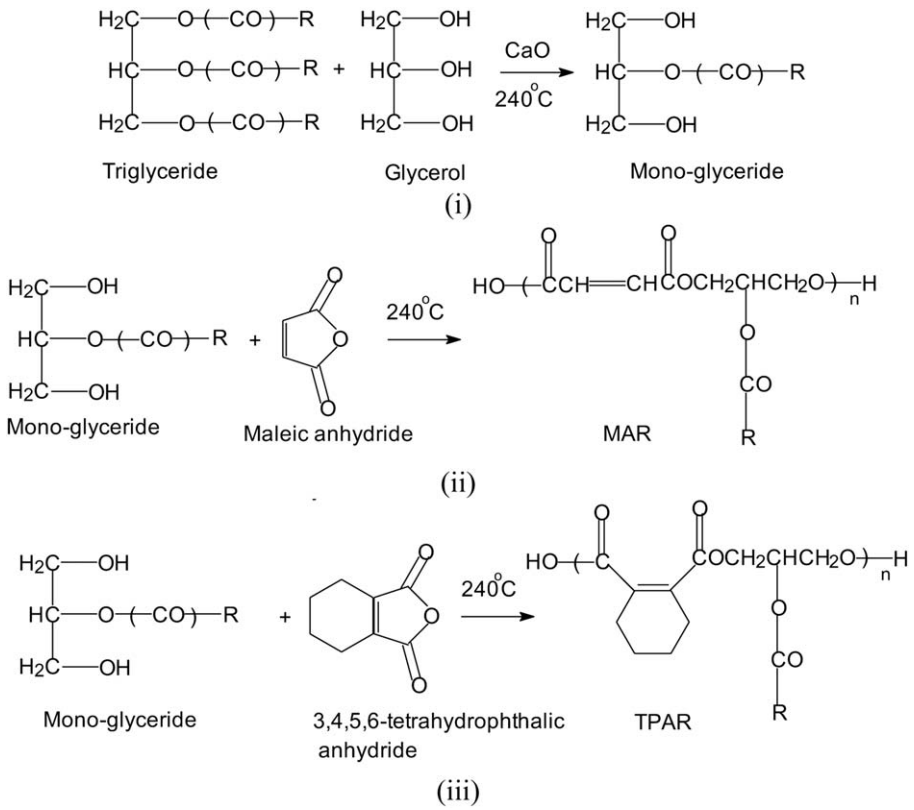


**Scheme 1.** Polyalkyds, maleic anhydride resin (MAR) and 3,4,5,6-tetrahydrophthalic anhydride resin (TPAR), preparation from palm oil through (i) alcoholysis and (ii,iii) esterification.

nanotubes (MWCNTs) were incorporated into the polyalkyds. In addition, an *in situ* technique during the polyesterification reaction was adopted to produce better interactions between the polymeric chain and the MWCNTs.

The incorporation of nanoparticles into thermosetting polymers is effective for improving the thermomechanical properties of the matrix. Various nanoparticles, such as silica, silver, and carbon black, have been used for different purposes, such as enhancing corrosion resistivity and improving antimicrobial activity and thermal and mechanical properties.[11–13] Just after carbon nanotubes (CNTs) were discovered by Iijima, research works based on CNTs and CNT-based composites increased rapidly.[14] The mechanical behavior, fabrication processes, and suitable applications have been discussed elaborately in previous articles.[15–17] The processing of nanotubes or nanoparticle incorporation into liquid resins or polymers has been found to be a tedious job for a uniform and even dispersion; this is considered to be a major shortcoming of this material.[18] The agglomeration or cluster formation of nanotubes is the reason for their uneven or poor dispersion into the polymer matrix. Weak van der Waals attractions between the carbon atoms and physical entanglements are thought to be the reasons behind the poor dispersion. There are different methods in practice for including nanotubes into polymers; these include sonication, extrusion, and calendaring. All of these methods may damage the CNTs, and this is probably the reason for the deteriorated properties in the resulting composites. Thus, the aim of this research work was to disperse CNTs by physical stirring with the help of a ultrasound bath and *in situ* reaction during the esterification process.

## EXPERIMENTAL

### Materials

Crude palm oil was kindly supplied by the Malaysian Palm Oil Board. Glycerol and calcium oxide were purchased from Aladdin Chemistry Co., Ltd. (Shanghai, China). Methyl ethyl ketone peroxide (MEKP) and 3,4,5,6-tetrahydrophthalic anhydride (molecular weight = 152.16 g/mol; chemical formula: $C_8H_8O_3$) was procured from Aladdin Chemical Corp. (Shanghai, China). Sulfuric acid was purchased from Fisher Scientific. Maleic anhydride was purchased from Acros. Cobalt naphthanate and styrene were purchased from Sigma Aldrich. MWCNTs with diameters of less than 8 nm, lengths of 10–30 μm, and carbon purities of 95% were purchased from Timesnano (China). Highly pure chemicals were used in this research as received without any modification.

### Synthesis of the Resin

Before resin preparation, the dehydration of palm oil was carried out to improve unsaturation. The increment in unsaturation was measured by the iodine value of the oil. The iodine value was measured by the method stated in ASTM D 554. For the dehydration process, 2% sulfuric acid was used in the presence of 2 wt % pumice. Nearly 50 g of crude oil was placed in a reactor with the said amount of sulfuric acid and pumice. The reaction time was maintained at 15 min, and we ensured an inert atmosphere by following nitrogen gas into the reaction

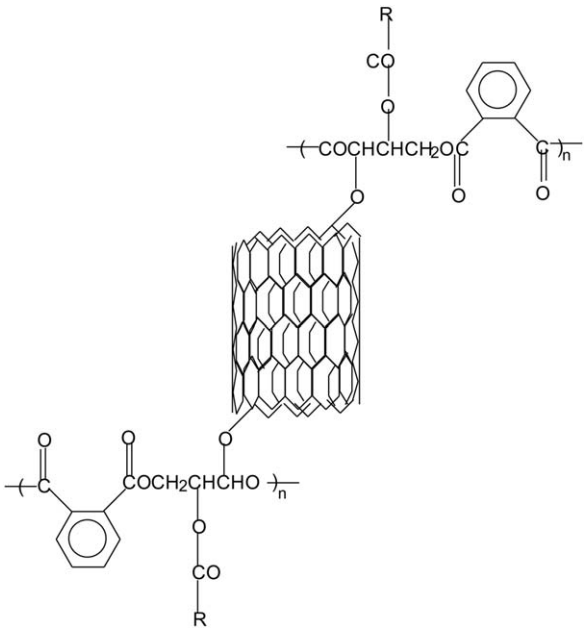

**Scheme 2.** Possible mechanism showing the interaction or interface of MWCNTs and alkyd resins.

chamber. The water generated from the reaction was collected through a Dean–Stark apparatus. The dehydrated oil was subjected to resin synthesis.

A four-necked glass vessel was used for the reactions. The vessel was placed in a magnetic heater, which was fixed with an automatic stirrer. An inert atmosphere was confirmed inside the reaction chamber by continuous flow of nitrogen gas. In the alcoholysis process, oil (32.2 g), glycerol (7.2 g), and catalyst (CaO; 0.04 g) were placed in the reaction chamber and heated for about 1.5 h at 240°C. The end point of the reaction was confirmed by the complete dissolution of the reaction products into methanol at a ratio of 1:3. After that, the reaction products were cooled down to 120°C. In the esterification process, different types of acid anhydrides, such as 3,4,5,6-tetrahydrophthalic anhydride (5 g) and maleic anhydride (12 g), were used with the reaction products of the alcoholysis. The temperature was maintained at 240°C for nearly 2 h. The end point of the reaction was confirmed by the measurement of the acid values of the products. After esterification, the reaction products were considered as liquid resins and kept for further testing. The reactions mechanism for alcoholysis and esterification is presented in Scheme 1.

**Curing Process and Preparation of the Nanocomposite Film**

The curing process of liquid resins involves the formation of linkages among the polymeric chains through the unsaturation present in resins. Likewise, in normal polymerization, the initiation of curing is required, and for that, an initiator must start the process. In this process, MEKP [4 parts per hundred grams of resin (phr)] and cobalt naphthalate (2 phr) were mixed with a definite amount of resin and 30 phr styrene. The mixture was then agitated manually at 60°C for 10 min. After that, the resins were poured onto Petri dishes and put in an oven for the curing process. The samples were checked frequently with a fingertip to trace the dryness and tackiness. Only free trace samples were considered as cured polymeric film for further characterization. The time for curing was recorded as the drying or curing time of the resins.

For nanocomposite film preparation, 0.5, 1.0, and 1.5 wt % MWCNTs were added with 1.0 g of resin with the said amounts of MEKP, cobalt naphthanate, and styrene. The sonication process was used for the mixing of the nanoparticles in an ultrasound bath for 2 h with 50% amplitude. For the *in situ* reaction, the optimum loading (evaluated during the mechanical performances) of the MWCNTs (1.0 wt %) was considered to add during the esterification reaction. The curing process of *in situ* reacted resin was followed as same as for the normal curing process described earlier. The possible interaction between the nanoparticles and polymer matrix is shown in Scheme 2.

**Characterization**

To examine the structural and functional groups, a Fourier transform infrared spectrophotometer (Thermo Scientific, model Nicolet Avatar 370DTGS) was used. The KBr method was used for the analysis with scanning ranges from 600 to 4000 $cm^{-1}$. The gloss of the cured resins was measured according to the ASTM D 523 method with a 60° gloss meter (model DR60A, China). The pencil hardness of the cured resin was measured with the help of a pencil hardness tester (model B-3084) on the scale of 6B to 6H of a standard set of pencils. The test was performed according to the ASTM D 3363 method. The scale of pencils for pencil hardness testing is presented in Figure 1.

A fresh portion of the cured film was also used to determine the tensile properties, including the tensile strength (TS), tensile modulus (TM), and elongation at break, with a universal testing machine (model Instron 4505) with a load cell of 5 kN. The method was followed according to ASTM D 638. The crosshead speed was fixed at 1 mm/min during the testing. TS and TM were reported for the mechanical properties of the film produced from different formulations.

X-ray diffraction (XRD) analysis was carried out with the help of a Rigaku Mini Flex II (Japan). The tube current of the X-ray generator and the working voltage were 15 mA and 30 kV, respectively. The other experimental details are reported elsewhere.[19] The surface of the films was observed by a field emission electron microscope (model JEOL JSM-7800F). The samples were coated with gold by a vacuum sputter coater before observation.

To determine the crosslinking density of the resins, the gel content was measured for a fixed amount of cured films. The Soxhlet extraction was used for the measurement. A finely meshed stainless steel net was used for wrapping up by the film. The extraction was carried out in hot acetone for 1 day. After that,

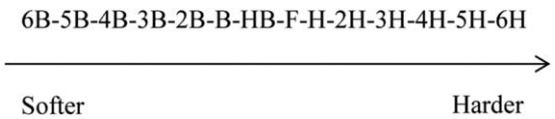


**Figure 1.** Scale of pencil hardness testing.

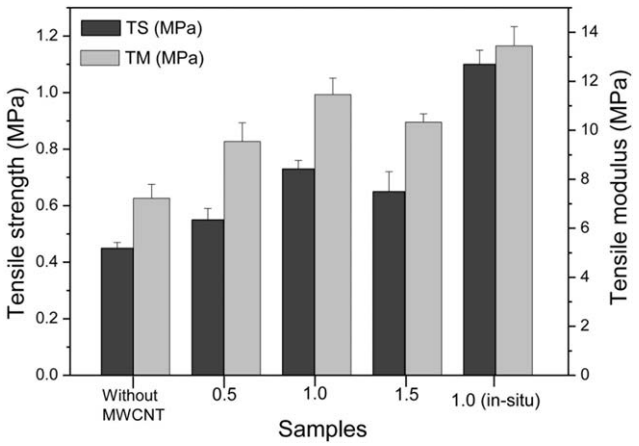


**Figure 2.** TS and TM values of different films.

the residues were dried in an oven, and their weights were recorded. The gel fraction of the cured films was determined by the following equation[20,21]:

$$\text{Gel fraction } (\%) = W_f / W_i \times 100 \quad (1)$$

where $W_f$ and $W_i$ are the weights after and before extraction, respectively.

We measured the swelling ratio of the gel by soaking the gel obtained from the gel fraction measurement testing in acetone for 24 h at 25°C. The swollen gel was pressed by two glass plates for 30 s after it was dried with filter paper. The weight ratio of the swollen gel to the gel before soaking was considered to be the swelling ratio[20]:

$$\text{Swelling ratio} = W_{sg} / W_g \quad (2)$$

where $W_{sg}$ and $W_g$ are the weights of the gel after and before soaking, respectively. The hydrophobicity of the films was measured by contact angle measurement with a contact angle meter (goniometer). A water droplet of about 5 $\mu$L was allowed to rest on the polymeric films, and images were captured. Fifteen images were analyzed for each sample with the help of contact angle software (model JY-82), and an average of 10 image results were computed to obtain the contact angle. The adhesion properties (crosscut) were measured according to the ASTM D 3359 method.

A thermogravimetric analyzer (TA Instruments, model TA-Q500) was used to determine the thermal decomposition behavior of the polymeric films. A sample of nearly 5 mg was placed in a platinum pan for testing. The heating rate was 20°C/min in the temperature range from 30 to 600°C. For the melting behavior, a differential scanning calorimeter (TA Instruments, model TA-Q1000) was used in a nitrogen atmosphere. An aluminum pan was used for testing at a heating rate of 10°C/min and in a temperature range from 30 to 410°C.

For chemical resistivity, about 0.5 g of each type of cured film was immersed in various chemicals, such as hydrochloric acid (5%), sodium hydroxide (5%), sodium chloride (5%), and distilled water, for 24 h at room temperature, and we measured the weight loss after the time period. Further, an extended period of time (24 h) was observed for the changes, and the weight loss was measured. A relative expression of the measurements, such as excellent (not affected), fair (less affected), and poor (affected), were used to indicate the chemical resistivity of the films on the basis of their weight losses.

## RESULTS AND DISCUSSION

### Tensile Properties

TS and TM of the films prepared without MWCNTs, with MWCNTs, and with MWCNTs reacted *in situ* are presented in Figure 2. The film prepared without MWCNTs showed a TS of 0.45 MPa, whereas the incorporation of 0.5 wt % MWCNTs brought about an improvement of nearly 22% (0.55 MPa). This may have been due to the mechanical entanglement of the nanoparticles by the polymeric chains; this improved the tensile properties. Furthermore, loading (1.0 wt %) enhanced the properties by 62% compared to the film prepared without MWCNTs. This improvement was attributed by the phenomenon where the presence of a sufficient amount of MWCNTs against of the volume of the polymeric chins was compatible. On the other hand, at 1.5 wt % loading, we found this to be discouraging in terms of TS. The value (0.65 MPa) was found to be lower compared to that of the film loaded at 1.0 wt %. This was probably due to large agglomeration, which may have acted as a stress concentration and subsequently reduced the tensile properties at lower stresses.[22] The deterioration of the properties was probably due to uneven distribution, which failed to create a strong physical bonding between the particles and the polymeric chains. Finally, the film filled with MWCNTs reacted *in situ* showed better tensile properties compared to the normally dispersed film loaded with 1.0 wt % MWCNTs. TS was found to be 1.1 MPa; this was 144 and 50% higher than those films prepared without MWCNTs and the normally prepared film loaded at same percentage of MWCNTs (1.0 wt %), respectively. This was probably due to the better mechanical entanglement of the nanotubes by the polymeric chain during the esterification process. A similar trend of behavior was observed for the case of TM. The film without MWCNTs showed a TM of 7.35 MPa, whereas a 0.5 wt % loading level enhanced the value to 9.54 MPa; this was further enhanced to 11.46 MPa at a 1.0 wt % loading. However, loading at 1.5 wt % decreased the value to 10.33 MPa, whereas *in situ* conditions at 1.0 wt % was found to be favorable for improving the TM from 11.46 to 13.45 MPa. The elongation at break of the films is listed in Table I. The elongation at break was found to be decreased because of the loading of the nanoparticles into the polymeric dispersion. The maximum elongation (15%) was shown by the film without MWCNTs, whereas the minimum elongation was shown by the film incorporated with 1.5 wt % MWCNTs (5%). The incorporation of 0.5 wt % reduced the elongation from 15 to 12%; further loading at 1.0 wt % decreased the value to 9%. However, *in situ* conditions were found to be favorable (11%) at the same loading because of the mechanical entanglement of the nanoparticles by the polymeric chains. The decrease was found to be drastic because the increases in the loading and maximum loading made the film almost brittle.

**Table I.** Elongation at Break of the Films

| Sample | Elongation at break (%) |
|---|---|
| Without MWCNTs | 15 |
| With 0.5 wt % MWCNTs | 12 |
| With 1.0 wt % MWCNTs | 9 |
| With 1.5 wt % MWCNTs | 5 |
| With MWCNTs reacted *in situ* | 11 |

### Pencil Hardness

The pencil hardness of the films prepared without MWCNTs, with MWCNTs (at different loading percentages), and with MWCNTs reacted *in situ* are tabulated in Table II. The film without MWCNTs showed a pencil hardness of category HB-type pencils, whereas the incorporation of 0.5 wt % allowed the film pass the testing of an H-type pencil. This was probably an effect of the physical entanglement of the polymeric films with the nanoparticles. Further loading (1.0 and 1.5 wt %) did not allow an increase in the hardness compared to the previous result, whereas the film with MWCNTs reacted *in situ* showed a higher value (2H) than the others. The lower mechanical properties of the nanocomposite film at higher fractions of loading were probably due to the stress concentration caused by the agglomeration of the nanotubes.[22] The highest properties in the *in situ* conditions were probably due to the better physical bonding between the nanoparticles and the polymeric chains of the polyalkyds.

### Structural Properties

Shown in Figure 3 are the Fourier transform infrared (FTIR) spectra of different films prepared without MWCNTs, with MWCNTs, and with MWCNTs reacted *in situ*. The overall observations of the curves showed the physical homogenity of the films; this was important for the incorporation of the nanoparticles into the polymeric dispersion. As revealed, from the liquid resin without MWCNTs, the carbonyl groups were depicted in the absorbance peak around 1741 $cm^{-1}$. The peaks for the same in every curve were found to be close to 1740 $cm^{-1}$; this indicated the homogenity of the polymeric chain. The peaks around 2850 and 2920 $cm^{-1}$ originated from the C—H stretching vibrations of the MWCNTs; this was also found to be close to the same in the film without MWCNTs.[23] The changes were observed for the case of peaks around 1250 $cm^{-1}$. A diffused peak observed in the region of

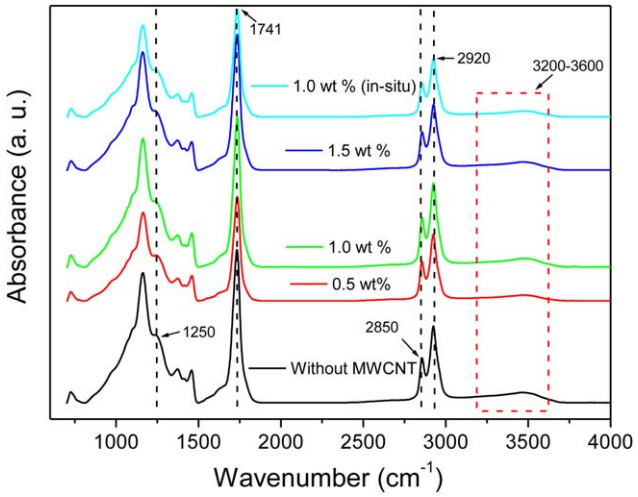


**Figure 3.** FTIR spectra of different films prepared without MWCNTs, with MWCNTs (at different loadings), and with MWCNTs reacted *in situ*. [Color figure can be viewed in the online issue, which is available at wileyonlinelibrary.com.]

1250 $cm^{-1}$ of the solid films from the liquid resins may have been due to the curing process and the incorporation of nanoparticles. Overall, no significant chnage was obsevred in the analysis; this may imply the absence of any chemical interactions beween the polymer and MWCNTs.[24]

Figure 4 shows the XRD patterns of different films loaded at different percentages of MWCNTs, without MWCNTs, and with MWCNTs reacted *in situ*. The plot shows curves for the intensity versus the scattering angle. The crystallinity, *d*-spacing, crystalline size, and crystallinity values are enlisted in Table III. A scattering angle ($2\theta$) of 19.77° for the film without MWCNTs, was observed probably because of the crystalline and amorphous regions of the polyalkyd resin, as shown by the medium sharp peak. The diffused portion of the curve was found to be sifted to 19.86, 20.65, 20.06, and 20.23 with the incorporation of MWCNT loadings of 0.5, 1.0, and 1.5 and MWCNTs reacted *in situ*, respectively; this was indexed by the (002) planes of the MWCNTs. The crystallinity was found to decrease from 45.76 to 31.46% with the loading of 0.5 wt % MWCNTs, whereas a further loading (1.0 wt %) increased the value from 31.46 to 37.76%. The decrease in the crystallinity was probably due to the incorporation of MWCNTs, which may have disturbed the regular arrangement of the polymeric chins. However, *in situ*

**Table II.** Pencil Hardness of Various Types of Cured Resins

| Pencil type | Without MWCNTs | 0.5 wt % MWCNTs | With 1.0 wt % MWCNTs | With 1.5 wt % MWCNTs | With MWCNTs reacted *in situ* |
|---|---|---|---|---|---|
| 2B | Pass | Pass | Pass | Pass | Pass |
| B | Pass | Pass | Pass | Pass | Pass |
| HB | Pass | Pass | Pass | Pass | Pass |
| F | Fail | Pass | Pass | Fail | Pass |
| H | Fail | Fail | Pass | Fail | Pass |
| 2H | Fail | Fail | Fail | Fail | Pass |

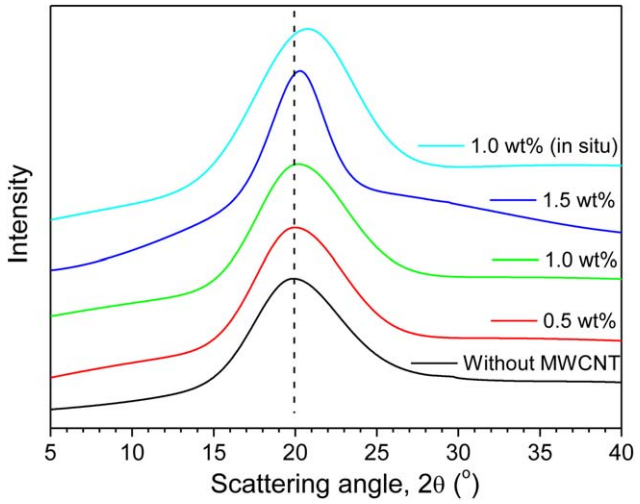


**Figure 4.** XRD diffractograms of different polymeric films prepared without MWCNTs, with MWCNTs (at different loadings), and with MWCNTs reacted *in situ*. [Color figure can be viewed in the online issue, which is available at wileyonlinelibrary.com.]

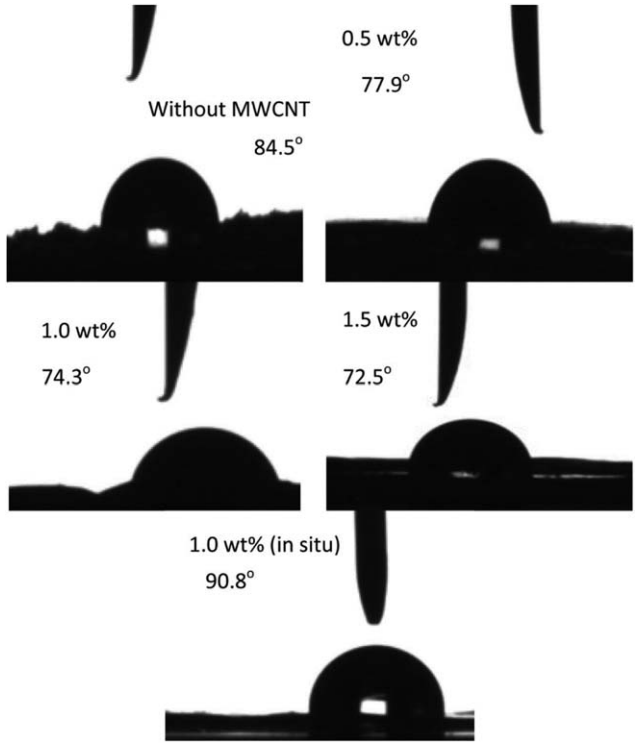


**Figure 5.** Contact angles of different polymeric films without MWCNTs and with MWCNTs.

conditions were also found to be favorable for increasing the crystallinity by 2%. The increment was probably due to the better entanglement of the nanotubes by the polymer chain, which was due to esterification process. The *d*-spacing was found to be 4.44 Å for the case of the film without MWCNTs, whereas the values of the films incorporated with MWCNTs were 4.29, 4.46, 4.42, and 4.39 Å, respectively. The crystalline sizes were found to be 13.65 and 13.98, 13.56, 13.18, and 21.5 nm for the films produced without MWCNTs; with MWCNTs at loadings of 0.5, 1.0, and 1.5 wt %; and with MWCNTs reacted *in situ*, respectively.

**Surface Properties**

Figure 5 shows the contact angle images of different films prepared without MWCNTs, with MWCNTs (at different loading percentages), and with MWCNTs reacted *in situ*. The contact angle of the film prepared without MWCNTs was found to be 84.5°, whereas films with MWCNT loadings of 0.5, 1.0, and 1.5 wt % showed values of 77.9, 74.3, and 72.5°, respectively. Furthermore, the film with MWCNTs reacted *in situ* showed a contact angle value of 90.8°. This was probably due to the changes in the surface chemistry of the films prepared with different percentages of MWCNTs.[25] The hydrophobicity of the films was found to decrease with loadings of MWCNTs up to 1.5 wt %. The incorporation of nanoparticles increased the wettability because of the hydrophilic nature of the MWCNTs. However, the better interfacial interaction and encapsulation of the nanoparticles with the polymers may have been possible reasons for the improved hydrophobicity of the film produced under *in situ* conditions.

The gloss properties were measured for different films prepared without and with MWCNTs. The results are listed in Table IV. The gloss was measured at 60° for the films. The film without MWCNTs showed a gloss value of 80; this was found further to improve with the incorporation of MWCNTs. The gloss values were found to be 83, 87, and 88 for the cases of films loaded with 0.5, 1.0, and 1.5 wt % MWCNTs, respectively. The *in situ* reacted film showed the highest gloss of 92. A gloss value more than 85 is considered high, values between 70 and 85 are standard, values from 40 to 70 are termed *semi*, and values from 15 to 40 are designated as low.[26]

The adhesion properties of the different films without and with MWCNTs are listed in Table IV. The adhesion was found to be 100% for the films prepared without MWCNTs and with MWCNTs loaded at 0.5 and 1.0 wt %. The properties for the

**Table III.** XRD Parameters for Different Types of Resins

| Resin type | Peak position (2$\theta$) | *d* (Å) | Crystalline size (nm) | Crystallinity (%) |
|---|---|---|---|---|
| Without MWCNTs | 19.77 | 4.44 | 13.65 | 45.76 |
| With 0.5 wt % MWCNTs | 20.65 | 4.29 | 11.98 | 31.46 |
| With 1.0 wt % MWCNTs | 19.86 | 4.46 | 13.56 | 37.76 |
| With 1.5 wt % MWCNTs | 20.06 | 4.42 | 13.18 | 37.47 |
| With MWCNTs reacted *in situ* | 20.23 | 4.39 | 21.50 | 39.11 |

**Table IV.** Gloss, Gel Content, Swelling Ratio, and Adhesion Properties of Different Resins

| Resin type | Gloss (60°) | Gel content (%) | Swelling ratio | Adhesion (%) |
|---|---|---|---|---|
| Without MWCNTs | 80 | 95 | 1.14 | 100 |
| With 0.5 wt % MWCNTs | 83 | 95 | 1.12 | 100 |
| With 1.0 wt % MWCNTs | 87 | 96 | 1.10 | 100 |
| With 1.5 wt % MWCNTs | 88 | 95 | 1.30 | 98 |
| With MWCNTs reacted *in situ* | 92 | 98 | 1.07 | 100 |

1.5 wt % loaded film were a little lower than those of the others. This was because of the high percentage of MWCNTs. Thus, a value of up to 1.0 wt % MWCNTs was found to be compatible for the adhesion properties, whereas greater loadings may have caused a disturbance in the adhesion properties. The polymeric unsaturated chain may have been attacked by atmospheric oxygen during adhesion progress; this probably disturbed the higher loading of the nanotubes. The drying time was recorded as 3 h 50 min for the film without MWCNTs; this increased to 4 h 7 min for the film loaded with 0.5 wt % MWCNTs. The increment of the drying time was probably due to the presence of MWCNTs. The films prepared with 1.0 and 1.5 wt % MWCNTs showed drying times of 4 h 12 min and 4 h 20 min, respectively. On the other hand, *in situ* conditions

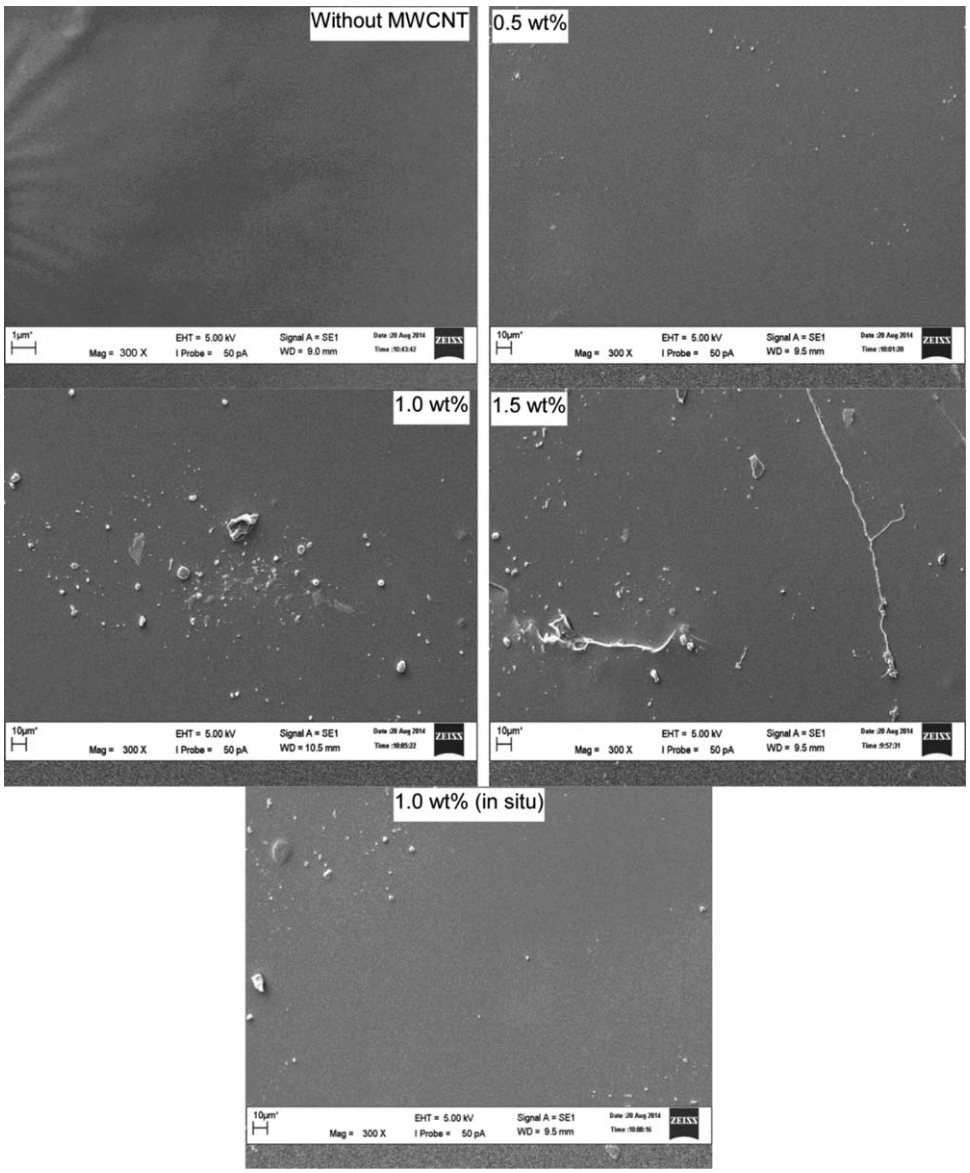


**Figure 6.** Surface morphology of the polyalkyd and polyalkyd films filled with different percentages of MWCNTs.

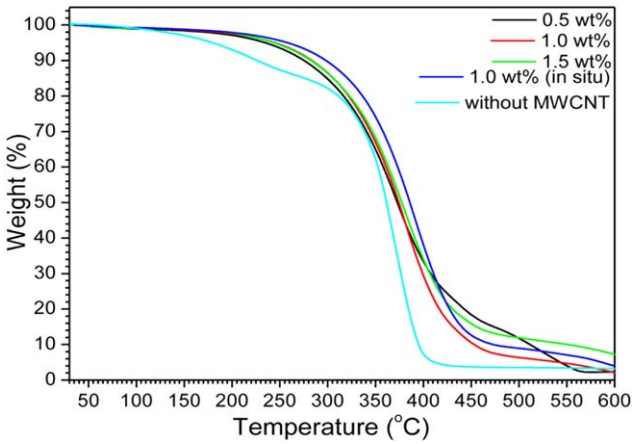


**Figure 7.** Weight–temperature curves for different films prepared without MWCNTs, with MWCNTs (at different loadings), and with MWCNTs reacted *in situ*. [Color figure can be viewed in the online issue, which is available at wileyonlinelibrary.com.]

showed the drying time (4 h 10 min); this was similar to the normally loaded film at a 1.0 wt % MWCNT loading.

Figure 6 shows the image of the surface of the different films produced without MWCNTs and with MWCNTs loaded at different percentages and with *in situ* conditions. The surface of the films were found to be smooth for the case of the film without nanoparticles and the 0.5 wt % loaded film, whereas the 1.0 and 1.5 wt % loaded films and the *in situ* reacted film showed comparatively rougher surfaces because of the particle dispersion. The surface of the 1.0 wt % loaded film showed some coagulation and agglomeration, which swelled the film surface and made it rough. Further loading at 1.5 wt % was found to produce the worst dispersion compared to the loaded films. The rupture and brittleness was apparent on the surface of the 1.5 wt % loaded film. The increase in the brittleness and the reduction of the elongation of the film loaded at 1.5 wt % was correlated with the surface roughness and poor dispersion. However, the *in situ* reacted film was also found to be rough, but the swelling was not visible, although few spots of coagulation and uneven distribution were also observed.

### Crosslinking Density

The swelling properties or the gel fraction values are sometimes important for the measurement of the crosslinking density of the polymers through qualitative measurements.[27–29] The comparative analysis of the crosslinking density of the polymers can be predicted from the gel content and the swelling ratio. The gel contents of different polymeric films produced without MWCNTs and with MWCNTs (loaded at different weight percentages and under *in situ* conditions; Table IV) were determined. The gel content was found to be 95% for the case of the film without MWCNTs, whereas the loading of MWCNTs did not significantly affect the gel content, which was found to be in the range 95–96%. On the other hand, the *in situ* reacted film showed the highest gel content, which was 98%. The swelling ratio of the films showed a similar trend as the gel content. The values for the swelling ratios were found to be 1.14, 1.12, 1.10, 1.30, and 1.07 for the case of the film prepared without MWCNTs and 0.5, 1.0, and 1.5 wt % for the films with MWCNTs reacted *in situ* (Table IV).

### Thermal Properties

The weight–temperature and derivative weight–temperature plots from the thermogravimetric analysis are illustrated in Figures 7 and 8, respectively. From the graphs, the thermal stability and degradation profile of various cured films prepared without MWCNTs, with MWCNTs (at different loading percentages), and with MWCNTs reacted *in situ* were analyzed and discussed. From the analysis, the weight loss around 1–2 wt % after 100°C was probably due to the removal of adhered moisture from the films. The removal of moisture and weight loss from that was confirmed by the isothermal heating of the polymers at 110°C for 2 h; this indicated the same amount of weight loss without any change in the chemical structure, as observed by FTIR spectroscopy. The incorporation of the MWCNTs enhanced the onset degradation for all of the films, as indicated in Figure 6. We found that the initiation of the degradation was found to be 350°C for the film without MWCNTs. The incorporation of nanoparticles increased the onset temperature ($T_{onset}$) to 352°C, and further loading at 1.0 wt % improved the onset temperature to 355°C. Loading at 1.5 wt % resulted in degradation at 352°C, whereas the loading of MWCNTs reacted *in situ* showed degradation at 355°C.

The incorporation of CNTs was found to be effective in improving the thermal stability of the polymers, as revealed from the previous research. For example, the onset degradation temperature of polypropylene was enhanced by 16 and 34°C with the inclusion of 0.5 and 1.0 wt % CNTs, respectively.[30] The improvement was also observed for the cases of poly(vinyl acetate) and poly(methyl methacrylate) with the incorporation of different percentages of MWCNTs.[31,32] Table V shows the thermal properties of different films based on MWCNTs and without MWCNTs. The residues after 600°C for all of the samples were found to increase with the loading of CNTs. The maximum residue, 7%, was observed for the 1.5 wt % loaded film. As shown in Figure 7, the maximum peak temperature ($T_{max}$) values were found to

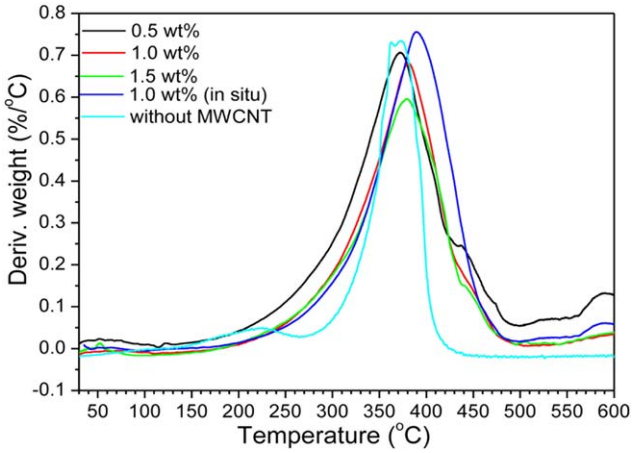


**Figure 8.** Derivative weight–temperature curves for different films produced without MWCNTs, with MWCNTs (at different loadings), and with MWCNTs reacted *in situ*. [Color figure can be viewed in the online issue, which is available at wileyonlinelibrary.com.]

**Table V.** Thermal Properties of Different Resins

| | $T_{onset}$ (°C) | $T_{max}$ (°C) | Residue (%) | $T_m$ (°C) |
|---|---|---|---|---|
| Without MWCNTs | 350 | 377 | 2 | 375 |
| With 0.5 wt % MWCNTs | 352 | 377 | 3 | 380 |
| With 1.0 wt % MWCNTs | 355 | 384 | 4 | 387 |
| With 1.5 wt % MWCNTs | 352 | 382 | 7 | 377 |
| With MWCNTs reacted *in situ* | 355 | 392 | 4 | 390 |

$T_m$, melting temperature; $T_{max}$, maximum peak temperature; $T_{onset}$, onset temperature.

be 377, 377, 384, 382, and 392°C. Thus, the thermal stability of these resins was found to be high enough to be used for any type of high-temperature-sustained application.

The differential scanning calorimetry thermograms of the films are illustrated in Figure 9. From the graph, a general idea was obtained about the melting temperature and the interaction between the MWCNTs and polymers; this led to information about the mechanical properties of the nanocomposite films. The thermosetting resins showed a broad region close to the melting point, as observed from the endothermic peaks. It was clear from the graphs that the incorporation of MWCNTs enhanced the melting temperature, whereas the *in situ* reacted particles enhanced the interfacial adhesion between the fibers and polymers, as confirmed by the shift in the melting points to a higher value compared to that of the film without MWCNTs. The melting temperature was found to be at a maximum (390°C) for the film prepared under *in situ* conditions, whereas the film prepared without MWCNTs and that prepared with 0.5, 1.0, and 1.5 wt % MWCNT loadings showed melting temperatures of 375, 380, 387, and 377°C, respectively. The order of thermal stability of the films was in good accordance with the observed mechanical properties of the films. The highest melting point of the *in situ* reacted film was probably due to the better interfacial interaction between the MWCNTs and the polymeric chains compared to that of the others.[33]

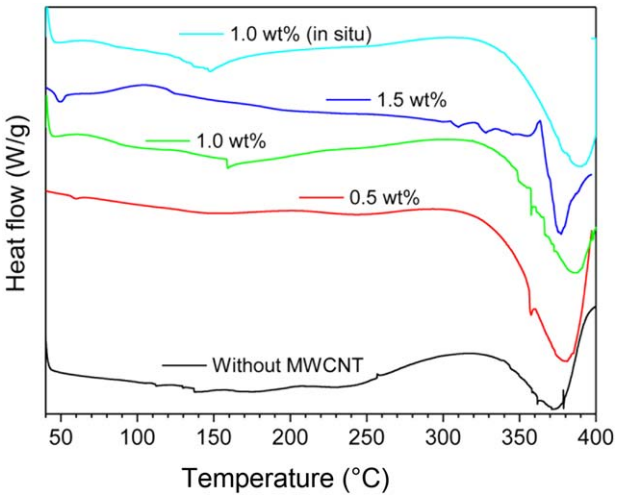


**Figure 9.** Differential scanning calorimetry thermograms for different films prepared without MWCNTs, with MWCNTs (at different loadings), and with MWCNTs reacted *in situ*. [Color figure can be viewed in the online issue, which is available at wileyonlinelibrary.com.]

### Chemical Resistivity

The performances of the chemical resistivity of various films prepared without MWCNTs, with MWCNTs at different loadings, and with MWCNTs reacted *in situ* are reported. Table VI shows the chemical resistivity performances of the films. The chemical resistivity for all of the films was found to be excellent for distilled water, brine solution, and hydrochloric acid solution. For the same period of time (24 h), the behavior against the sodium hydroxide solution was also found to be similar, except for the film prepared under *in situ* conditions. The film prepared under *in situ* conditions showed excellent chemical resistivity against the sodium hydroxide solution. When the period was extended to 48 h, the results were found to be different, and the films were affected with the variation of time. For 48 h of immersion, almost all of the films were found to be unaffected in distilled water and brine solution, but films prepared with MWCNTs were found to be slightly affected by the hydrochloric acid solution and fairly affected by the sodium hydroxide solution. On the other hand, among the films, the *in situ* reacted MWCNT-based film showed the best resistivity. It was unaffected in sodium hydroxide and other solutions for 48 h of immersion. This was thought to be due to better interfacial interaction and entanglement of the nanoparticles by the polymeric chains. Moreover, the presence of strong intramolecular and intermolecular secondary

**Table VI.** Chemical Resistivity of the Cured Resins

| | Solution | Without MWCNTs | With 0.5 wt % MWCNTs | With 1.0 wt % MWCNTs | With 1.5 wt % MWCNTs | With MWCNTs reacted *in situ* |
|---|---|---|---|---|---|---|
| 24 h | Distilled water | Excellent | Excellent | Excellent | Excellent | Excellent |
| | 5% HCl (aqueous) | Excellent | Excellent | Excellent | Excellent | Excellent |
| | 5% NaOH (aqueous) | Poor | Fair | Excellent | Fair | Excellent |
| | 5% NaCl (aqueous) | Excellent | Excellent | Excellent | Excellent | Excellent |
| 48 h | Distilled water | Excellent | Excellent | Excellent | Excellent | Excellent |
| | 5% HCl (aqueous) | Poor | Fair | Excellent | Excellent | Excellent |
| | 5% NaOH (aqueous) | Poor | Poor | Fair | Poor | Excellent |
| | 5% NaCl (aqueous) | Excellent | Excellent | Excellent | Fair | Excellent |

forces, namely, hydrogen bonding, polar–polar bonding, and mutual crosslinking, were thought to be additional reasons behind the higher chemical resistivity of the MWCNT-filled film.[34] The improvement of the chemical resistivity of polymeric fibers in organic solvents due to the incorporation of MWCNTs was also observed in a previous study.[35]

## CONCLUSIONS

Palm-oil-based alkyd resins and their films incorporated with MWCNTs at various percentages were prepared and characterized. The effects of the incorporation of different percentages (0.5, 1.0, and 1.5 wt %) of MWCNTs were evaluated in terms of the mechanical, structural, thermal, and morphological properties. The properties of the MWCNT-loaded films were compared to those of films without MWCNTs. The beast loading was selected on the basis of the tensile properties of the formulated films. We found that 1.0 wt % MWCNTs showed the best loading percentages in terms of the tensile properties. Furthermore, *in situ* conditions during esterification were considered for a 1.0 wt % loading of MWCNTs, and the results were also compared with the others to determine the effects of the *in situ* conditions. The properties of the *in situ* reacted MWCNT-based film were found to be motivational and suggested the fabrication for polyalkyd-based nanocomposite film for high-temperature stability and better chemical resistivity.

## ACKNOWLEDGMENTS

The Universiti Malaysia Pahang is highly appreciated for providing financial support through research grants PGRS 130357 and RDU 140332.

## REFERENCES

1. Islam, M. R.; Beg, M. D. H.; Jamari, S. S. *J. Appl. Polym. Sci.* **2014**, *131*, 40787.
2. Islam, M. R.; Beg, M. D. H.; Gupta, A. *J. Thermoplast. Compos. Mater.* **2014**, *27*, 909.
3. Miao, S.; Wang, P.; Su, Z.; Zhang, S. *Acta Biomater.* **2014**, *10*, 1692.
4. Guner, F. S.; Yagci, Y.; Erciyes, A. T. *Prog. Polym. Sci.* **2006**, *31*, 633.
5. Aigbodion, A. I.; Okieimen, F. E.; Obazee, E. O.; Bakare, I. O. *Prog. Org. Coat.* **2003**, *46*, 28.
6. Dutta, N.; Karak, N.; Dolui, S. K. *Prog. Org. Coat.* **2004**, *49*, 146.
7. Boruah, M.; Gogoi, P.; Adhikari, B.; Dolui, S. K. *Prog. Org. Coat.* **2012**, *74*, 596.
8. Ali, M. A.; Ooi, T. L.; Salmiah, A.; Ishiaku, U. S.; Ishak, Z. A. M. *J. Appl. Polym. Sci.* **2001**, *79*, 2156.
9. Saravari, O.; Phapant, P.; Pimpan, V. *J. Appl. Polym. Sci.* **2005**, *96*, 1170.
10. Issam, A. M.; Cheun, C. Y. *Malaysian Polym. J.* **2009**, *4*, 42.
11. Zhang, W.-G.; Li, L.; Yao, S.-W.; Zheng, G.-Q. *Corros. Sci.* **2007**, *49*, 654.
12. Dolatzadeh, F.; Moradian, S.; Jalili, M. M. *Corros. Sci.* **2011**, *53*, 4248.
13. Dinha, D. A.; Huib, K. S.; Huia, K. N.; Cho, Y. R.; Zhou, W.; Hong, X.; Chun, H.-H. *Appl. Surf. Sci.* **2014**, *298*, 62.
14. Iijima, S. *Nature* **1991**, *354*, 56.
15. Thostenson, E. T.; Ren, Z.; Chou, T. W. *Compos. Sci. Technol.* **2001**, *61*, 1899.
16. Liu, J.; Fan, S. S.; Dai, H. *J. MRS Bull.* **2004**, *29*, 244.
17. Choi, W. B.; Bae, E.; Kang, D.; Chae, S.; Cheong, B. H.; Ko, J. H.; Lee, E.; Park, W. *Nanotechnology* **2004**, *15*, S512.
18. Gibson, R. F.; Ayorinde, E. O.; Wen, Y.-F. *Compos. Sci. Technol.* **2007**, *67*, 1.
19. Mina, M. F.; Beg, M. D. H.; Islam, M. R.; Nizam, A.; Alam, A. K. M. M.; Yunus, R. M. *J. Polym. Eng. Sci.* **2014**, *54*, 317.
20. Chowdhury, M. N. K.; Alam, A. K. M. M.; Dafader, N. C.; Haque, M. E.; Akhtar, F.; Ahmed, M. U.; Rashid, H.; Begum, R. *Biomed. Mater. Eng.* **2006**, *16*, 223.
21. Chowdhury, M. N. K.; Ismail, A. F.; Beg, M. D. H.; Hegde, G.; Gohari, R. J. *New J. Chem.* **2015**, *39*, 5823.
22. Shokrieh, M. M.; Saeedi, A.; Chitsazzadeh, M. *J. Nanostruct. Chem.* **2013**, *3*, 20.
23. Li, Q. H.; Zhou, Q. H.; Deng, D.; Yu, Q. Z.; Gu, L.; Gong, K. D.; Xu, K. H. *Trans. Nonferrous Met. Soc. China* **2013**, *23*, 1421.
24. Chen, Z. K.; Yang, J. P.; Ni, Q. Q. *Polymer* **2009**, *50*, 4733.
25. Kim, S.; Kafi, A. A.; Bafekpour, E.; Lee, B.-I; Fox, B.; Hussain, M.; Choa, Y.-H. *J. Nanomater.* **2015**, Article ID 130270. http://www.hindawi.com/journals/jnm/2015/130270/. Accessed on May 20, 2015.
26. Richart, D. S. *Powder Coat.* **1999**, *2*, 25.
27. Oh, K. S.; Oh, J. S.; Choi, H. S.; Bae, Y. C. *Macromolecules* **1998**, *31*, 7328.
28. Mtshali, T. N.; Krupa, I.; Luyt, A. S. *Thermochim. Acta* **2001**, *380*, 47.
29. Omidian, H.; Hashemi, S.-A.; Askari, F.; Nafisi, S. *Iran. J. Polym. Sci. Technol.* **1994**, *3*, 115.
30. Jose, M. V.; Dean, D.; Tyner, J.; Price, G.; Nyairo, E. *J. Appl. Polym. Sci.* **2007**, *103*, 3844.
31. Minoo, N.; Lin, T.; Tian, W.; Dai, L.; Wang, X. *Nanotechnology* **2007**, *18*, 1.
32. Zhang, H.; Wang, Z. G.; Zhang, Z. N.; Wu, J.; Zhang, J.; He, J. S. *Adv. Mater.* **2007**, *19*, 698.
33. Guo, S.; Zhang, C.; Wang, W.; Liu, T.; Tjiu, W. C.; He, C.; Zhang, W.-D. *Polym. Polym. Compos.* **2008**, *16*, 471.
34. Dutta, S.; Karak, N. *Pigment Resin Technol.* **2007**, *36*, 74.
35. Minus, M. L.; Chae, H. G.; Kumar, S. *Macromol. Chem. Phys.* **2009**, *210*, 1799.